Supplementary Figures and Legends

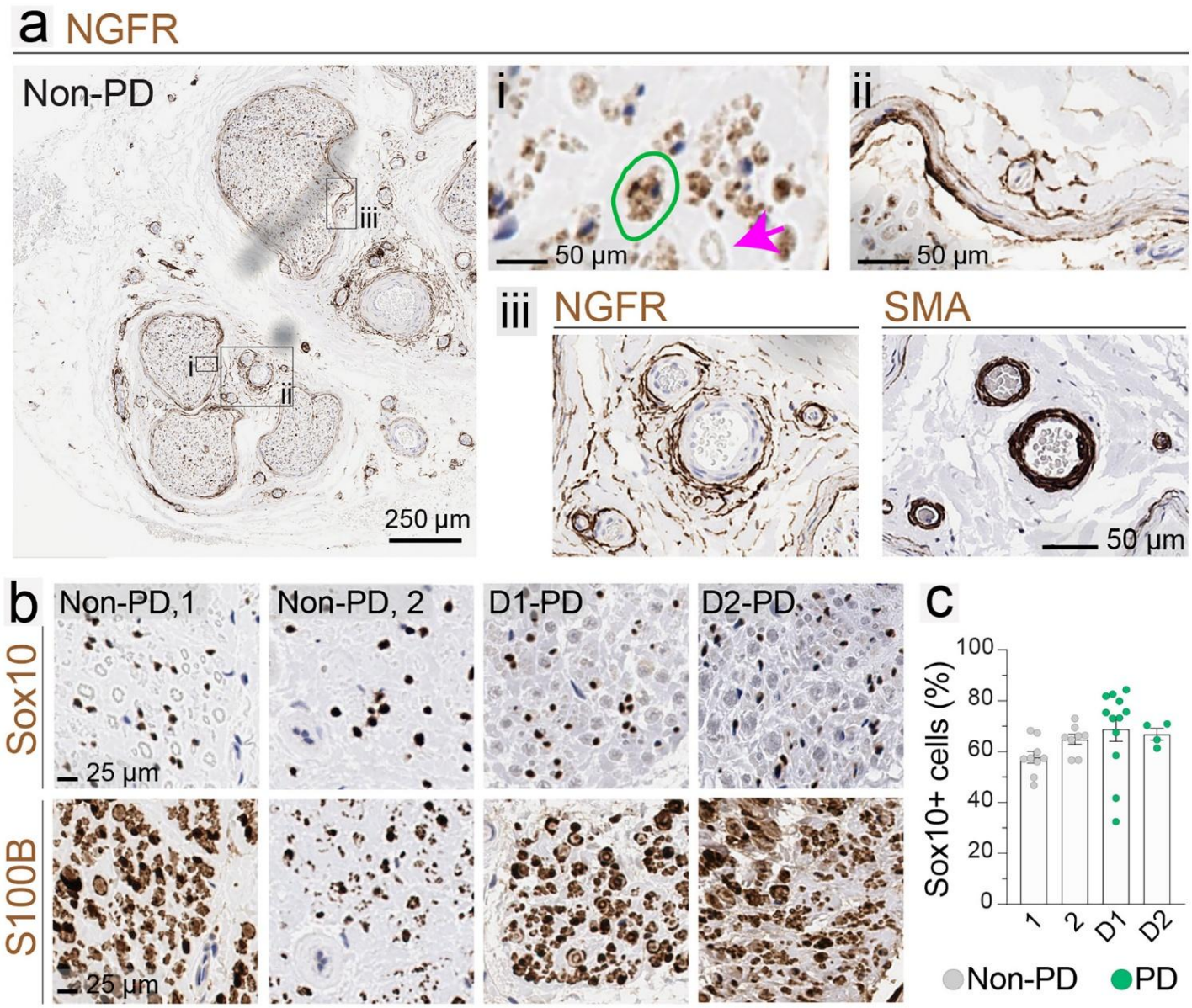

Supplementary Figure 1: **Sural nerve analysis from participants with PD compared to non-Parkinsonian (Non-PD) controls. (a)** Representative images of a non-PD sural nerve immunostained to detect NGFR+ cells (anti-NGFR, brown). Low magnification image of fascicles embedded within a large epineurial layer containing numerous BVs. Zoomed-in images show in detail NGFR negative, myelinating-SCs (pink arrow) and NGFR positive Remak SCs (green circle) (i); NGFR+ perineurial cells (ii), and NGFR+ epineurial fibroblasts (iii) surrounding BVs (stained with anti-SMA). **(b, c)** Sox10 expression (nuclear staining) was roughly equivalent in the sural nerves of non-PD and PD participants indicating invariant SC density in these nerves.

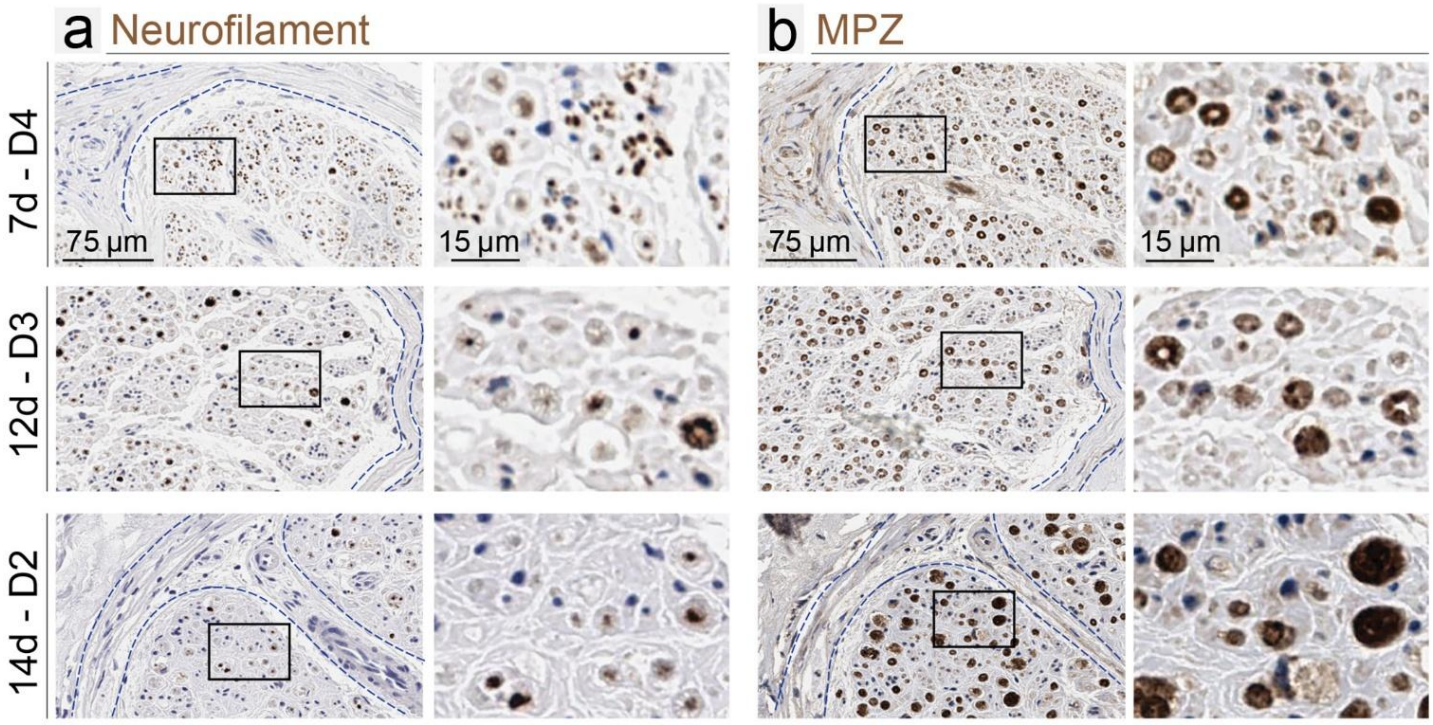

Supplementary Figure 2: **Evidence of temporal changes in axon and myelin degradation after injury. (a, b)** Representative images of NF and MPZ staining of injured nerves harvested at 7 (donor-4), 12 (donor-3), and 14 (donor-2) days post-axotomy. Observe the slow progression of axon degeneration and the relative conservation of the ring-like structures of myelin sheaths at 7- and 12-days post-injury.

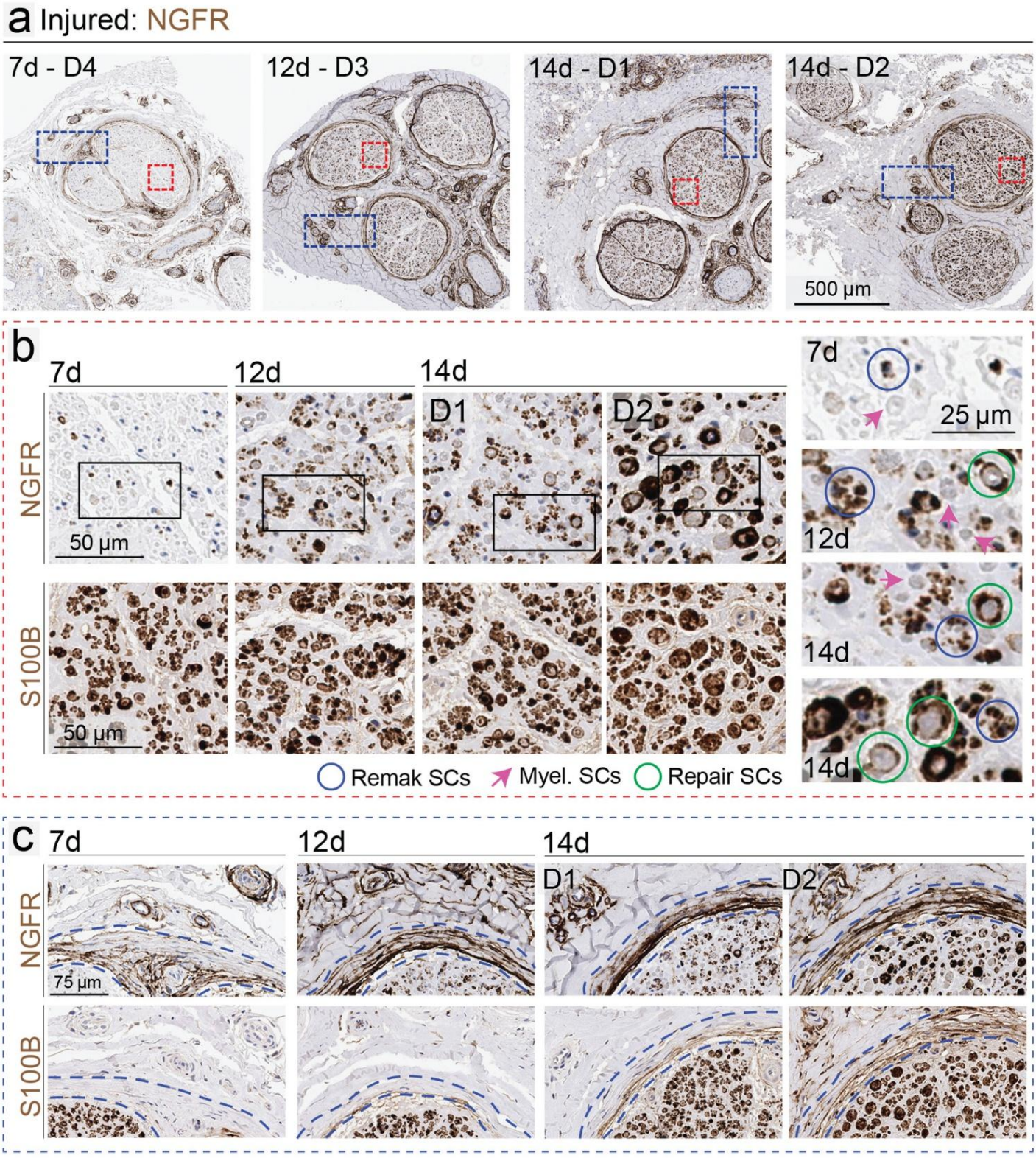

Supplementary Figure 3: **Evidence on the temporal progression of injury-induced NGFR expression in SCs and connective tissue cells. (a)** Low magnification images of NGFR-stained (brown) injured nerves at 7 (donor 4), 12 (donor 3), and 14 (donors 1 and 2) days post-axotomy. **(b)** Comparison of NGFR and S100B expression levels inside injured fascicles showcasing high NGFR expression in repair SCs (green circles). **(c)** Representative epi- and perineurial areas denoting strong NGFR levels in perineurial (blue dotted lines) and epineurial cells as soon as 7 days post-axotomy. S100B expression in perineurial cells was observed at 14 days post-axotomy.

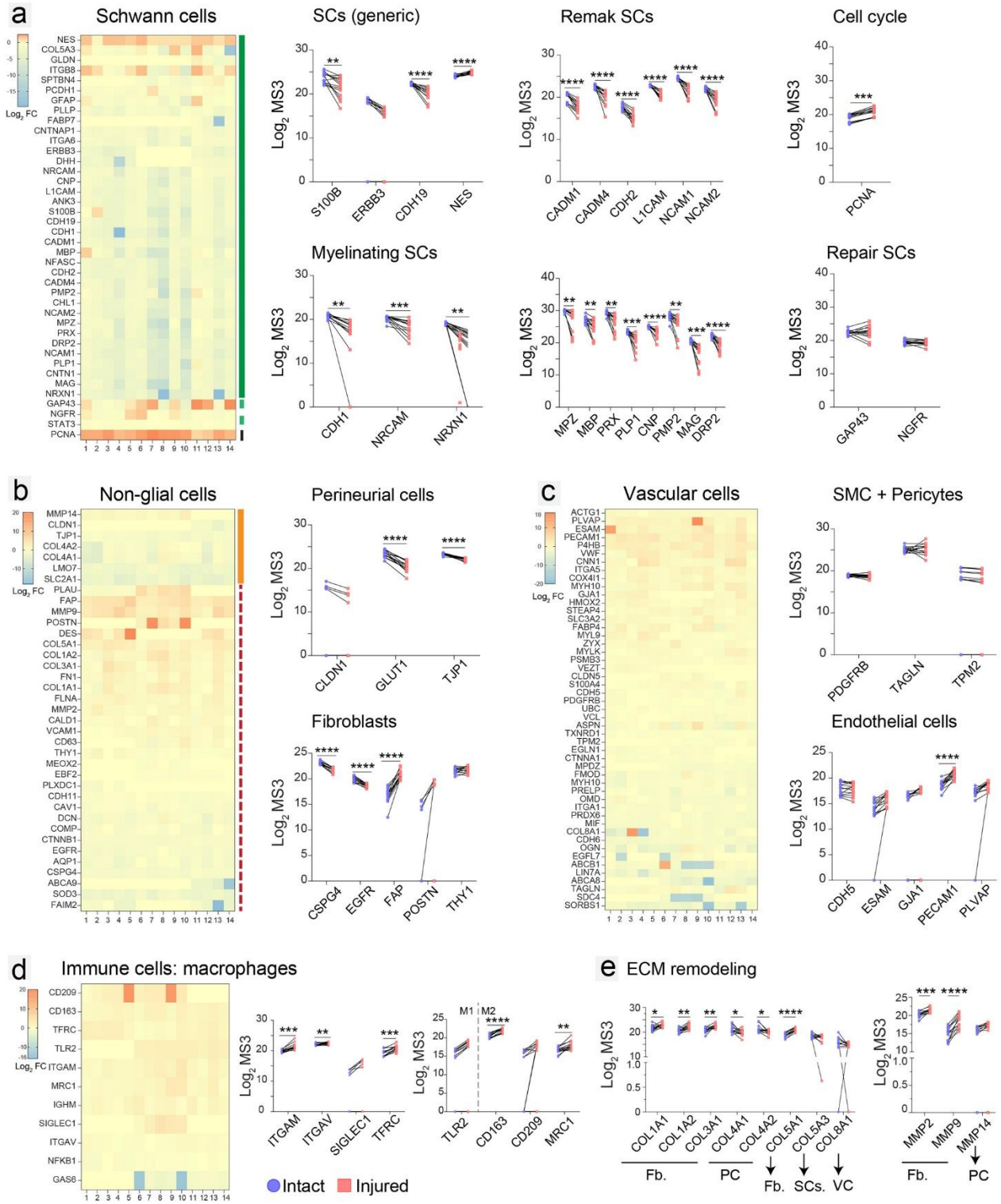

Supplementary Figure 4: Injury-dependent changes in the expression levels of selected proteins typical of SCs, vascular, immune, and connective tissue cells. (a-d) Heatmaps (Log_2 FC) are shown along with selected proteins from the categories and subcategories described in Figs. 8-9, in each clinical trial participant (n=14) as indicated in the figure. Plots show the normalized levels (Log_2 MS3) from representative proteins in each category. Only macrophage-associated proteins were detected despite the broad representation of immune cell genes evidenced at the transcript level. **(e)** Collagen and MMP isoforms (ECM remodeling) are shown separately. The cell phenotype in which each protein is prevalently expressed has been indicated in the figure, as follows (Fb.: fibroblasts, PC: perineurial cells, SCs: Schwann cells, and VC: vascular cells).

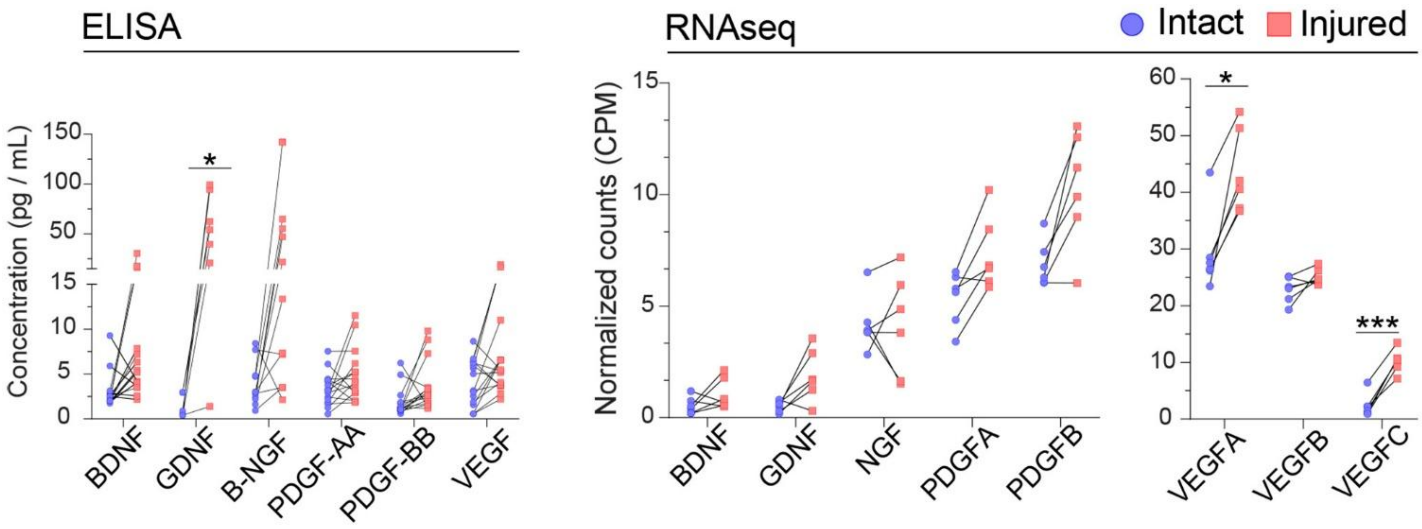

p value	BDNF	GDNF	NGF	PDGFB	PDGFA	VEGF	VEGFA	VEGFB	VEGFC
ELISA	0.0783	0.0149	0.0776	0.1010	0.1010	0.1010			
RNAseq	0.2308	0.0685	0.9709	0.1065	0.0660		0.0131	0.0587	0.0002

Supplementary Figure 5: Injury-dependent changes in the expression levels of neurotrophins and other growth factors. The figure contains results from ELISA immunodetection assays for secreted growth factors of interest (as indicated in the figure) in intact and injured nerve samples from 15 clinical trial participants. The transcript levels for these factors were detectable by RNAseq in 6 clinical trial participants (left panel, data shown in normalized counts or CPMs), (Welleford et al. 2020) but were not abundant enough for detection by mass spectrometry. Protein data (ELISA) was available from Chau et al (2022), (Chau et al., 2022a). P values are indicated in the table.